NJC

Accepted Manuscript

This is an *Accepted Manuscript*, which has been through the Royal Society of Chemistry peer review process and has been accepted for publication.

Accepted Manuscripts are published online shortly after acceptance, before technical editing, formatting and proof reading. Using this free service, authors can make their results available to the community, in citable form, before we publish the edited article. We will replace this *Accepted Manuscript* with the edited and formatted *Advance Article* as soon as it is available.

You can find more information about *Accepted Manuscripts* in the Information for Authors.

Please note that technical editing may introduce minor changes to the text and/or graphics, which may alter content. The journal's standard Terms & Conditions and the Ethical guidelines still apply. In no event shall the Royal Society of Chemistry be held responsible for any errors or omissions in this *Accepted Manuscript* or any consequences arising from the use of any information it contains.

ROYAL SOCIETY OF CHEMISTRY

www.rsc.org/njc

New Journal of Chemistry RSCPubli

shing

ARTICLE

Visible-Emitting Hybrid Sol-Gel Materials Comprising Lanthanide Ions: Thin Film behaviour and Potential Use as Phosphors for Solid-State Lighting

Cite this: DOI: 10.1039/x0xx00000x

Received 00th January 2012,
Accepted 00th January 2012

DOI: 10.1039/x0xx00000x

www.rsc.org/

Xiaoguang Huang,[a,b] Gaël Zucchi,*[,b] Jacqueline Tran,[b] Robert B. Pansu,[c] Arnaud Brosseau,[c] Bernard Geffroy,[d] François Nief[a]

The synthesis and characterization, as well as the film-forming and luminescent properties of four visible-emitting hybrid organic-inorganic sol-gel materials are reported. They show thermal stability up to 165°C. Deposition conditions were optimized to coat these materials as homogeneous and transparent thin films (~50 nm) of smooth surface, as probed by AFM. They were specifically designed to emit the three primary colours. The blue-emitting material **1** was made up of a polyfluorene derivative embedded into a silica matrix, while the green (**2**) and red (**3**)-emissive materials comprise the Tb^{III} and Eu^{III} ions bound to the matrix, respectively. The films showed relatively high emission quantum yields efficiencies, with values of 19% (blue), 46% (green), and 21% (red). The three emitters were used to design a single emissive material (**4**) that showed emission from yellow-green to blue in a wide range of excitation wavelengths (254-380 nm). In particular, white light was obtained for excitation 340 nm. The Eu^{III} material was investigated as a potential phosphor coated on an UV LED, and primary investigations on its stability under operating conditions are reported.

1. INTRODUCTION

Sol-gel processing is a smart way to process functional hybrid organic-inorganic silica materials that exhibit several outstanding physicochemical properties. Among these are a good mechanical strength and chemical and thermal stability associated to an excellent transparency. These features make them particularly interesting for optical applications.[1-3] In addition, sol-gel processing allows for the deposition of materials of high purity and chemical homogeneity as the molecular precursors can be easily purified, homogeneously dispersed in the reactant medium, and the gel can directly be coated. Such ambient temperature liquid deposition conditions are compatible with the coating of layers of desirable shapes on various substrates in addition of being viable on an industrial scale. In consequence, sol-gel chemistry is widely used in ceramics and glass industries. In particular, the possibility of processing the materials as thin films (thicknesses in the range 1-1000 nm) is of a much higher interest than using the materials as powders, especially because of their excellent transparency and homogeneity.

Thanks to pure and specific colours of emission (except for Ce^{III}), a great interest has been devoted to the use of the trivalent lanthanide ions (Ln^{III}) for optical applications. Especially, the large increase in the light absorption cross-section by the "antenna effect"

makes the insertion of lanthanide ions surrounded by suitable organic chromophores in inorganic glasses a way of choice for designing efficient light-emitting materials. Because of soft reaction conditions, and especially the reasonable reaction temperature, organic-containing molecules can be inserted within the sol-gel matrix. The design of thin films made up of materials comprising lanthanide complexes encapsulated in different organic[4-6] or inorganic[7-11] matrices is not frequently described in academic literature with respect to studies on bulk materials. It is however a field of investigation that is attracting a growing interest as it allows the determination of the properties of the final processed material that will be used for practical applications. Also, encapsulating a luminescent complex within a sol-gel matrix often resulted in an increase in the luminescence efficiency due to an efficient shielding of the emissive ion by the inorganic matrix from non-radiative deactivation such as O-H oscillators.[12-14] It was also observed that encapsulation in sol-gel glasses increased the photostability of lanthanide complexes under UV irradiation.[15-17]

Lanthanide complexes can be inserted into an inorganic silica matrix in three ways, namely impregnation, doping or immobilization.[18] The impregnation method is a physical doping where the lanthanide complexes penetrate the interspaces of the silica framework. The major drawback is the instability of the material due to the clustering of the complex. The doping method consists in dispersing the molecular complex in the inorganic matrix, while immobilization refers to a covalently linkage of the luminescent complex to the matrix. Two families of organic-inorganic materials originate from these doping methods:[19] class I gathers together hybrid materials resulting from the "conventional" doping of a molecule into a matrix. The molecular complexes interact with the inorganic matrix through weak interactions such as van der Waals forces or hydrogen bonding. This results in binary complex/matrix systems.[20,21] Class II is formed of materials with the dopant being covalently linked to the Si-O network, resulting in single materials. This latter immobilization method has been shown to lead to materials with improved thermal stability and luminescence efficiency.[22-26] The luminescence of these materials could be further improved by increasing the content of the emitter without self-quenching, thanks to a better dispersion of the coordinating sites within the matrix.[18,27]

In the work reported herein, we aimed at taking advantage of the coordination of the Eu^{III} and Tb^{III} ions to the matrix to form homogeneous thin films and we expected to benefit from the positive influence of the matrix on the luminescence properties of these. The photostability of such hybrid luminescent materials is usually checked by exposing powders or films to a xenon lamp. We proposed to investigate it by following the luminance over time of a LED chip coated with the Eu-material. This experiment represents a way close to real operating conditions to investigate the Eu^{III} material as a red phosphor for Solid-State Lighting (SSL).

Experimental section

Materials. Tetraethoxysilane (TEOS), 9,9-dihexyl-2,7-dibromofluorene, tetraethylammonium hydroxide (20% in H_2O), 9,9-di-*n*-octylfluorene-2,7-diboronic acid bis(pinacol) ester, tri(*p*-tolyl)phosphine, terbium(III) acetylacetonate hydrate (99.9%), ([Tb(acac)$_3$].xH_2O), and palladium(II) acetate, ([Pd(OAc)$_2$]), were purchased from Aldrich.
5-(*N*,*N*-bis-3-(triethoxysilyl)-propyl)ureylphenanthroline (Phen-Si_2),[28] Poly(9,9-dihexylfluorene-*alt*-9,9-dioctylfluorene) (PF(6,6-*alt*-8,8)),[29] and europium thenoyltrifluoroacetylacetonate ([Eu(tta)$_3$].xH_2O)[30] were synthesized as previously described.

Synthesis and thin films preparation. *PF-sol-gel (1)* . TEOS (50 mg) was mixed with ethanol (42 mg), and then triethylamine (50 µL) was added to the above mixture under magnetic stirring to initiate the hydrolysis and condensation reaction. The molar ratio of TEOS/ethanol/H_2O was 1:4:4. After stirring for 3 h, a THF solution containing PF(6,6-*alt*-8,8) (3 wt%) was added to the sol. The mixture was stirred at 50 °C for 4 h, afterwards the solution was spin-casted on a glass substrate at 3000 rpm for 30 sec. Drying the film at 100 °C for 2 days yielded the final film of the material. The material used for IR measurements was isolated as a powder by drying the gel after 3 days of ageing.

Tb-sol-gel (2). TEOS and 5-*N*,*N*-di(amidopropyltriethoxysilane)-1,10-phenanthroline (Phen-Si_2) were mixed with ethanol, and then water acidified with HCl vapours to pH = 5 was added to the above mixture under magnetic stirring to initiate the hydrolysis and condensation reaction. The molar ratio of Phen-Si_2/TEOS/ethanol/H_2O was 1:4:16:16. After stirring for 3 h, an ethanol solution containing [Tb(acac)$_3$].xH_2O (9 mg, the molar ratio of [Tb(acac)$_3$].xH_2O/TEOS was 1:4) was added to the sol, and the mixture was stirred at 50 °C for 4h. The final thin films and powder were formed as described for *PF-sol-gel.*

Eu-sol-gel (3). TEOS and Phen-Si_2 were mixed with ethanol, and then water acidified with HCl vapours (pH = 2) was added to the above mixture under magnetic stirring until the pH reaches a value of 2 to initiate the hydrolysis and condensation reaction. The molar ratio of Phen-Si_2/TEOS/ethanol/H_2O was 1:4:16:16. After stirring for 3 h and when the pH was 5, an ethanol solution containing an appropriate amount of the complex [Eu(TTA)$_3$].xH_2O (the molar ratio of Eu-TTA/TEOS was 1:4) was added to the sol. The mixture was stirred at 50 °C for 4 h.

PF-Tb-Eu-sol-gel (4). The hybrid material containing PF(6,6-*alt*-8,8) and covalently doped with the Tb^{III} and Eu^{III} ions was prepared by first heating at 50°C for 30 min TEOS (16 mg, 0.7 mmol), ethanol, and water in a molar ratio 1:4:4. Water acidified with HCl vapours to pH = 5 was added to the above solution. Then, an ethanolic solution containing Phen-Si_2, [Tb(acac)$_3$].xH_2O, and [Eu(tta)$_3$].xH_2O in a molar ratio 7:6:1 was added. After 3 hours of stirring, a THF solution (1.5 mg in 0.2 ml) of PF(6,6-*alt*-8,8) was added. After 4 hours of ageing, the solution was spin-casted on a glass substrate at 3000 rpm for 30 sec. Drying the film in a oven for 2 days yielded the final film. The material was isolated as a powder by drying the gel after 3 days of ageing.

Physico-chemical characterization

*Fourier transform infrared (FTIR) spectroscopy***.** Measurements were performed with a Bruker Equinox 55 spectrometer on samples conditioned as KBr pellets.

*Thermal analysis***.** Thermogravimetic Analyses (TGA) were made on a Netzsch STA 409 PC Luxx® analyser under a N_2 atmosphere at a rate of 5°C/min.

Profilometry. Thicknesses were measured with a Dektak profilometer.

Luminescence spectroscopy. Spectra were recorded on a Jobin Yvon Fluoromax4 spectrometer. Quantum yields measurements were performed with a Horiba Jobin Yvon Fluorolog3 spectrofluorometer equipped with an integration sphere according to published procedures.[31] The error was evaluated to be ± 12% after 4 measurements on different samples. The luminescence decay were measured with a nanosecond photolysis setup (Edinburgh Instruments) with an excitation at 280 nm and a detection at 488 nm with a fast photomultiplier.

Atomic Force Microscopy. Atomic Force Microscopy (AFM) measurements were performed with a dimension 3000 microscope from Digital Instruments.

Photostability measurements. Measurements were performed in an inert N_2 atmopshere with a home-made instrumental setup that will be described elsewhere.

Results and Discussion

Synthesis

The synthetic approach used herein to insert the lanthanides into the materials was the functionalization of the 1,10-phenanthroline ligand to transform it into a silane precursor. This strategy was preferred as it allows both a mixing at the molecular level of the precursors and the lanthanide ions are covalently bound to the inorganic matrix. As described above, this should eliminate problems of phase separation, inhomogeneous dispersion, and optical quenching of the dopants. Also, binding the lanthanide ion to the matrix generally leads to an improvement of the lanthanide emission.

Infra-red spectra of the four materials are reported in Figure 1. They show the characteristic absorption bands of a Si-O-Si framework. The δ (Si-O-Si) vibrations appear between 440 and 462 cm^{-1}, the ν_s (Si-O) vibrations are found in the range 785-792 cm^{-1}, and absorptions due to the ν_{as} (Si-O) vibrations appear between 1072 and 1090 cm^{-1}.[32] Broad bands corresponding to ν_{O-H} (most probably coming from Si-OH groups) andν_{N-H} (coming from the phenanthroline ligands) show maxima around 3550 and 3300 cm^{-1}, respectively, while the absorption of the C-H (CH_2) vibrations absorb in the range 3050-2780 cm^{-1}.[33] A better differentiation between **1** and the three other materials can be made by analyzing the 1450-1800 cm^{-1} region. The $\nu_{C=O}$ (phenanthroline) and ν_{C-O} (β-diketonates)[34] appear at 1711 and 1602 cm^{-1} in the lanthanide-containing materials, while no absorption is observable in this region for the polyfluorene material.

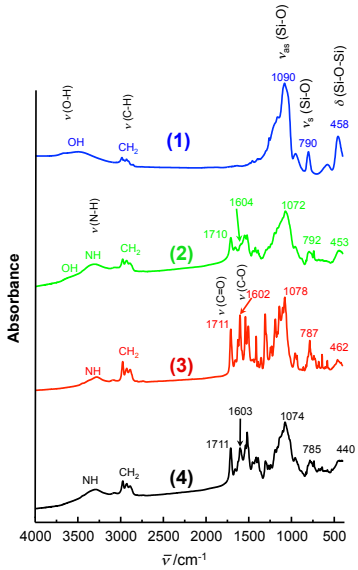

Figure 1. Infra-red spectra of **1** (blue), **2** (green), **3** (red), and **4** (black).

Thermal properties

Thermogravimetric analysis was performed on the materials in order to probe their stability over temperature in the range 30-600°C. The curves are reported in Figure 2. Comparison between the two curves recorded for a sample of **2** dried at 100°C for 2 h and for two days, respectively, shows that a considerable amount of adsorbed water can effectively be eliminated from the materials. The second general observation is that the materials are stable up to 165°C, which is a good point in a view of the targeted applications. Mass losses are observed between 165 and 500°C. They are attributed to the successive loss of tta and/or acac ligands and the 1,10-phenanthroline organic part for the lanthanide-containing materials. In the case of **1**, the mass loss observed at 425°C is due to the loss of the alkyl chains.[29]

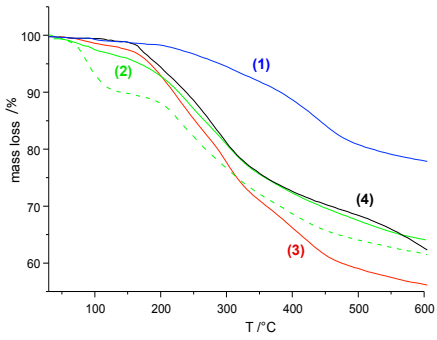

Figure 2. TGA curves for **1** (blue), **2** dried for 48h (green), **2** dried for 2h (green, dashed line), **3** (red), and **4** (black).

Thin film morphology

The surface morphology of the luminescent sol-gel thin films has been investigated by AFM. This is of importance in view of using them as emissive coatings. The images that have been obtained on films of thickness of 50 nm are reported in Figure 3. All surfaces have been found to be relatively smooth and homogeneous. A thin film of **1** (Figure 3a) shows a surface morphology with average (R_a) and rms (R_q) roughnesses of 0.47 and 0.59 nm, respectively. The peak-to-valley height amounts to 2.5 nm. The surface of **2** (Figure 3b), **3** (Figure 3c), and **4** (Figure 3d) are also homogeneous with R_a values of 0.23, 0. 28 nm and 0.66 nm, and R_q values of 0.30, 0.35, 0.81 nm, respectively. The peak-to-valley height was found to be 2.0, 2.5, and 3.0 nm for **2**, **3**, and **4**, respectively. In addition to the absence of phase separation, the important information brought by these AFM images is that the films are crack-free.

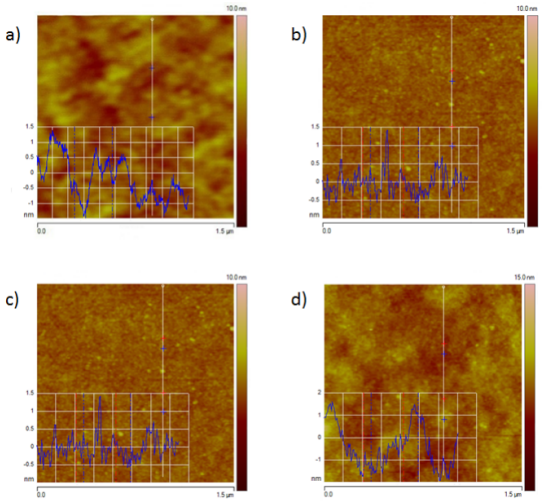

Figure 3. Topographic AFM images of **1** (a); **2** (b); **3** (c), and **4** (d). Onsets show the topographic profiles that were taken along the lines.

Photophysical properties

The absorption spectra of thin films coated on quartz substrates are reported on Figure 4. They show the characteristic $\pi\rightarrow\pi^*$ electronic transitions of the β-diketonates and phenanthroline ligands for the lanthanide-containing materials as well as the $\pi\rightarrow\pi^*$ transition observed in a pure thin film of polyfluorene.[29] More precisely, the absorption spectrum of **1** shows a main band with a maximum at 378 nm and a full-width-at-half height (FWHH) of 5132 cm^{-1}. The absorption spectrum of **2** shows a band with a maximum at 276 nm (FWHH of 4712 cm^{-1}) corresponding to absorption of both the acac and phenanthroline ligands, while that of **3** shows the typical $\pi\rightarrow\pi^*$ transition of the thiophene ring (maximum at 274 nm) with a shoulder at 291 nm that can be attributed to the $n\rightarrow\pi^*$ electronic transition of keto carbonyl and enol carbonyl groups of the tautomers. A second band appears at 351 nm (FWHH of 5032 cm^{-1}) and corresponds to a $\pi\rightarrow\pi^*$ transition that originates from the conjugation along the whole tta ligands.[35] These bands also comprise a contribution of the phenanthroline ligand.[4] Finally, the absorption spectrum of **4** shows two distinguishable bands whose maxima are located at 273 and 350 nm, respectively. These two band envelopes are originating from the simultaneous absorption of the tta and phenanthroline ligands and that of the polyfluorene described above for the single-emitter-containing materials.

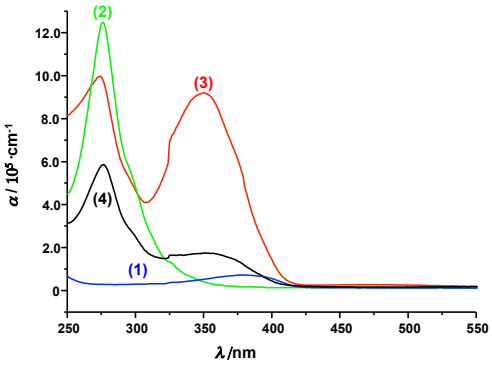

Figure 4. Normalized absorption spectra of thin films of **1** (blue), **2** (green), **3** (red), and **4** (black).

The excitation and emission spectra of **1**-**3** coated as thin films are reported in Figure 5. The excitation spectra are similar to the absorption spectra described above. This shows that, for the polyfluorene-containing material, the absorbing state is also the emitting state, and that for the Tb- and Eu-containing materials, an energy transfer occurs from the absorbing ligands to the lanthanide ion. The excitation spectrum of **2** shows two bands with maxima at 288 and 323 nm, corresponding to the phenanthroline and acac ligands, respectively, and that of **3** shows a main band with maximum at 360 nm and a shoulder around 288 nm, corresponding to the tta and phenanthroline ligands, respectively. The emission spectrum of **1** shows a structured band in the blue region with a maximum at 425 nm that corresponds to emission of the polyfluorene.[29] We did not observe any β-phase formation of the polyfluorene as recently described in ionogels.[36] When excited at 280 nm, the emission spectrum of **2** shows the $^5D_4\rightarrow{}^7F_J$ (J = 6-3) transitions of the Tb^{III} ion at 490, 546, 584, and 620 nm, respectively. The $^5D_4\rightarrow{}^7F_5$ transition is the most intense and thus responsible for the green emission of this material. Emission from both the $^5D_1$ and $^5D_0$ excited states of the Eu^{III} ion are observed in **3**. The former gives rise to a transition at 537 nm that only represents less than 0.3% of the overall europium emission. In consequence, it does not impact the optical properties of the material and will not be further discussed. The typical $^5D_0\rightarrow{}^7F_J$ (J = 0–4) transitions are observed with maxima at 579, 591, 611, 650, and 700 nm, respectively. The most intense is the $^5D_0\rightarrow{}^7F_2$ transition. The hypersensitive character of the latter allowed us to gain information on the symmetry of the local environment around the Eu^{III} ion.[37,38] In the present case, the predominance of the $^5D_4\rightarrow{}^7F_2$ transition is consistent with the Eu^{III} ion being in a low-symmetry site, which is in accordance with what should be expected in such heteroleptic complexes.[4,39] The ratio between the intensity of the $^5D_0\rightarrow{}^7F_2$ transition over that of the $^5D_0\rightarrow{}^7F_1$ transition is a good indicator of this low-symmetry. It amounts to 12 in the present case. Furthermore, the $^5D_0\rightarrow{}^7F_2$ transition represents 82% of the total Eu^{III} ion emission in the material, which is responsible of the monochromatic red emission of **3**. Emission of the three single-emitter-containing materials was observed in a wide range of excitation wavelengths belonging to the UV and ranging from 254 to 380 nm.

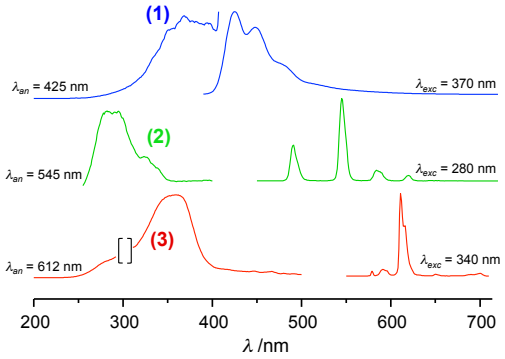

Figure 5. Excitation and emission spectra of thin films of **1** (blue), **2**(green), and **3** (red). The region in brackets has been deleted as it showed the Rayleigh band.

Material **4** was synthesized in order to use the simultaneous emissions of the three emitters to obtain a white-emitting coating. The emission spectrum of a thin film of **4** was found to depend on the excitation wavelength. Emission spectra recorded at different excitation wavelengths comprised in the 254-380 nm range are reported on Figure 6a, and the chromaticity diagram obtained after excitation in the UV region (254-380 nm) is reported in Figure 6b. Colours from yellow-green to blue were obtained when increasing the excitation wavelength. In particular, white light was obtained for an excitation wavelength of 340 nm. This is in accordance with the emissive behaviour of the single-emitter-containing materials described above and can be interpreted as follows. When the material is excited at higher energy, where absorption is mostly due to the β-diketonates, only emission of the Tb^{III} and Eu^{III} ions is observed. As the excitation wavelength is increased, the blue emission of the polyfluorene is becoming more intense, as its absorption increases. At excitation wavelengths close to visible light, only the polyfluorene becomes efficiently sensitized, as it is the only emitter that significantly absorbs at these wavelengths. This is corroborated by the excitation spectra that were recorded by analyzing the different specific emission bands (Figure 6c). When monitoring the polyfluorene emission at 425 nm where the Tb^{III} and Eu^{III} ions do not emit, the excitation spectrum corresponds to that of **1** with a maximum at 369 nm. When monitoring the $^5D_4\rightarrow{}^7F_{6,5}$ transition of the Tb^{III} ion, the excitation spectra show two bands with

maxima at 378 and 319 nm, respectively. The first band is due to the polyfluorene derivative as it still emits at these wavelengths. In addition, its relative intensity is higher when the analysis wavelength is set at 488 nm, a wavelength for which the emission of the polyfluorene derivative is most intense. The second band is due to the β-diketonates sensitizers. Finally, when monitoring the $^5D_0 \rightarrow {}^7F_{2,3,4}$ transitions of the Eu^{III} ion, we observed a band with a maximum at 340 nm due to the ttas, but also a relatively weakly intense band at 274 nm which can be attributed to the acac ligands. This shows that emission at 612, 543, and 700 nm is sensitized by the acac ligands. Indeed the $^5D_4 \rightarrow {}^7F_{3,2,1}$ transitions of the Tb^{III} ion also occur at these wavelengths. This can also be an indication of the sensitization of the Eu^{III} ion emission by acac ligands (see below).

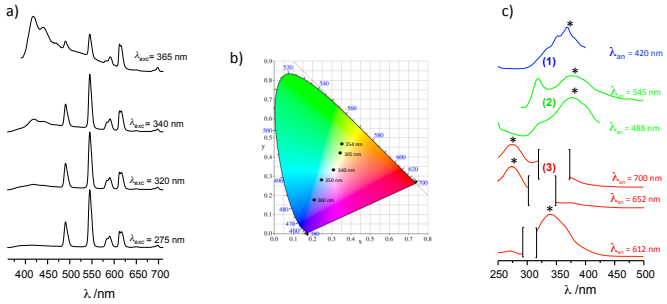

Figure 6. a) Emission spectra of a thin film of **4** at various excitation wavelengths; b) excitation spectra by monitoring different emissions (asterisks mark the wavelength used to normalized the spectra, and regions in brackets have been deleted as they showed the Rayleigh band); c) CIE chromaticity diagram of **4** as a function of the excitation wavelength.

Overall quantum yields obtained upon ligand excitation were determined for the four materials. Relatively high values were found for the single-emitter containing materials, as they amount to 19, 46, and 21 % for thin films of **1**, **2**, and **3**, respectively.

A value lower than 1% was measured for the overall quantum yield of a thin film of **4** after excitation at 340 nm. Also, the Eu^{III} and Tb^{III} emissions were found to be lower than those obtained in the single-emitting materials. In particular, the emission from the $^5D_4$ level was found to be relatively low with respect to that obtained in **2**. These relatively poor emissive properties of the Tb^{III} ion in this material were anticipated to result from two possible deactivation pathways of the $^5D_4$ level. We firstly envisaged an energy transfer from the Tb^{III} $^5D_4$ excited state to the Eu^{III} ion. The values found for the lifetimes of the $^5D_4$ and $^5D_0$ excited state in the single emitting materials and in **4** reported above could not allow us to conclude in an efficient Tb-to-Eu energy transfer. As a matter of fact, an efficient energy transfer would have led to a pronounced decrease of the lifetime of the $^5D_4$ (Tb) excited state level along with an increase of that of the $^5D_0$ (Eu) excited state in **4**.[40,41] The lifetimes of the $^5D_4$ level was found to be 120 µs in **2**, while a value of 99 µs was measured in **4**. Meanwhile, values of 356 and 117 µs where measured for the lifetime of the $^5D_0$ excited state in **3** and **4**, respectively. These values do not support an efficient Tb-to-Eu energy transfer. Another possibility is a ligand exchange occurring between the Tb^{III} and Eu^{III} ions during the synthesis that could result in the presence of $[Tb(acac)_x(tta)_yPhen]$ and $[Eu(acac)_n(tta)_mPhen]$ species. This would explain the sensitization of Eu^{III} by acac ligands under excitation at 274 nm. In such a case, the emitting ions would be complexed by less efficient sensitizers. In particular, the presence of tta ligands bound to Tb should led to an efficient back-energy transfer from the $^5D_4$ level to the ttas' triplet state as the two excited states are positioned at a similar energy (~ 20500 cm^{-1}).[42] As such a process is thermally activated, measurements as a function of temperature should show an increase of the Tb^{III} emission when decreasing the temperature.[43,39] To probe this, we measured emission spectra at variable temperature of a film of the composition 6 Tb: 1 Eu: 7 $PhenSi_2$: 28 TEOS. The intensity of the $^5D_4 \rightarrow {}^7F_{6,5}$ (Tb) and $^5D_0 \rightarrow {}^7F_2$ (Eu) transitions with temperature is reported in Figure 7. The emission intensity of the Eu^{III} ion did not show any dependence with temperature, while that of the Tb^{III} ion effectively decreased when increasing the temperature. More precisely, measurements report the luminescence intensity at constant excitation intensity. In this case, the signal is proportional to the luminescence yield. We assume that the excited states of the lanthanides are decaying through three paths: both radiative and non-radiative deactivation, and back transfer to the ligand. The deactivation rates associated to each process are labelled k_r, k_{nr}, and k_a, respectively, and the inverse of the luminescence rate is related to these deactivation rates by Eq. 1. The back-transfer process is thermally activated with an activation energy E_a (Eq. 2, k_a^0 is the radiative decay rate constant in absence of back transfer).

$$\phi = k_r/(k_r+k_{nr}+k_a) \qquad (1)$$

$$1/I \approx (1+k_{nr}/k_r+k_a^0/k_r \exp(-E_a/kT)) \qquad (2)$$

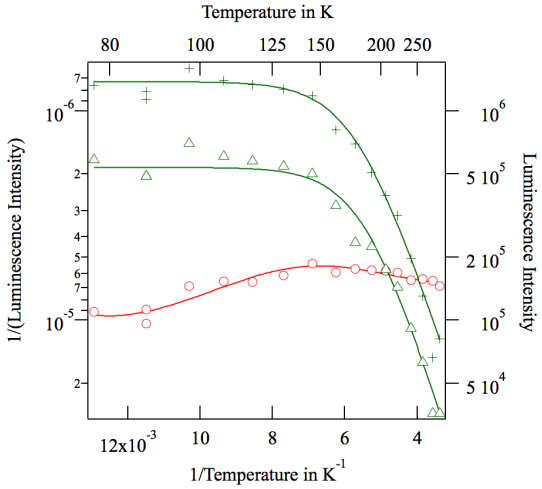

Figure 7. Intensity of the $^5D_4 \rightarrow {}^7F_6$ (Δ) and $^5D_4 \rightarrow {}^7F_5$ (+) transitions of Tb^{III} and that of the $^5D_0 \rightarrow {}^7F_2$ transition of Eu^{III} (o) with temperature in a film of composition 6 Tb:1 Eu:7 $PhenSi_2$:28 TEOS.

As can be seen from Figure 7, emission from the Tb^{III} ion is temperature dependant and follows the proposed model. We analyzed the $^5D_4 \rightarrow {}^7F_6$ and $^5D_4 \rightarrow {}^7F_5$ transitions and the fitting afforded values of 900 ± 30 cm^{-1} and 850 ± 25 cm^{-1} for E_a, respectively. These results led us to the conclusion that a back-energy transfer occurred with the Tb^{III} ion, and that tta sensitizers were coordinated to the Tb^{III} ion because of a ligand exchange that occurred during the synthesis.

The Eu^{III} material as a red phosphor for SSL

White light-emitting diodes are seen as the next generation of lighting as they present some advantages over other conventional lighting systems as they are relatively environment-friendly saving

of about 70 % in energy and considerably reducing CO_2 emission. The LED technology usually consists of combining a blue or near UV LED chip and a yellow emitting phosphor. However, this kind of light often suffers from a poor colour rendering index (CRI) due to the lack of the red component. Thus, red-emitting phosphors are worth to be developed. Among these, inorganic nitrides[44] and quantum dots[45] have been investigated. However, they have some drawbacks such as a high manufacturing cost resulting from high-temperature synthesis conditions for the former ones, and toxicity for the latter. Hybrid sol-gel materials comprising the Eu^{III} ion thus appear as an interesting alternative, especially as the red emission can be sensitized by near UV excitation (typically 350-400 nm). Within these lines, and because **3** strongly absorbs in the near-UV, its ability to act as a potential red phosphor for SSL was investigated. Very few reports deal with the use of hybrid lanthanide-containing materials as phosphors for near-UV LEDs,[45-49] their photostability was not studied under operating conditions. Usually, the photostability of such materials is investigated by exposing a film to a UV-emitting xenon lamp,[15,50-52] but it is not measured when the material is directly coated on the LED chip and illuminated by it. In order to get data close to operational conditions, we performed a preliminary experiment that is described hereafter. The material was coated on a commercial 390 nm-emitting LED chip. The resulting LED showed a bright red emission with CIE coordinates (0.65,0.34), figure 8 (insert). The luminance of the LED reached 400 cd/m^2 at a current of 4 mA. We chose to perform measurements with these conditions of luminance, as, usually, a computer display emits between 50-300 cd/m^2, and it is recommended that the luminance of a source of light used for lighting should not exceed 500 cd/m^2. Measurement of the ratio of the luminance L over the initial luminance (L_0 = 400 cd/m^2) over time under operating conditions in a nitrogen atmosphere is shown in Figure 8. After 10 hours of continuous operation, which roughly correspond to a day of office work, an interesting value of 83% of the initial luminance was retained. The EL spectrum recorded after this time still showed red emission with CIE coordinates of (0.60, 0.37). This indicates a relatively good stability of the colour, justifying the use of the Eu^{III} ion as emitter.

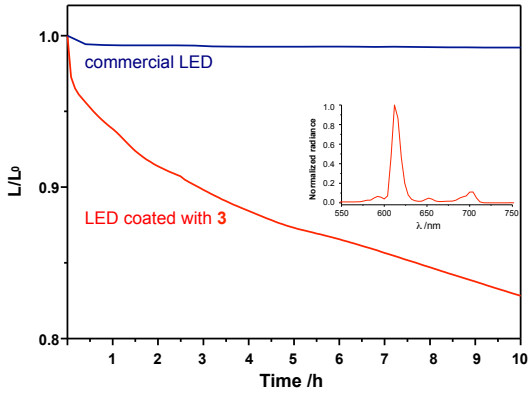

Figure 8. L/L_0 as a function of time of a UV-LED chip coated with **3**; L_0 is fixed at 400 cd/m^2 (see text) and the insert shows the initial EL spectrum.

Conclusions

Four luminescent hybrid organic-inorganic silica materials were synthesized and characterized by the means of FT-IR spectroscopy and thermal analysis. They were coated to obtain thin films of high homogeneity and with smooth surface that emit the three primary colours under near-UV excitation. The blue-, green-, and red-emissive materials containing a single emitter afforded coatings with good emission efficiencies. A film comprising the three dopants was found to emit from yellow-green to blue when excited in the range 254-380 nm. More often, colour change is obtained by changing the dopants ratio in such materials.[11,53,54] In particular, the material behaved as a single white-emitting film when excited at 340 nm. No noticeable interaction between the dopants could be evidenced, in particular no energy transfer was found to occur between the Tb^{III} and Eu^{III} ions. However, it was shown that ligands exchange took place during the synthesis. This resulted in the coordination of sensitizers with lower efficiencies on the Tb^{III} and Eu^{III} ions, and subsequent lower emission of these ions.

These results are encouraging as they show that single emissive thin layers with excellent properties in terms of surface quality and homogeneity can be easily obtained from solution deposition techniques that are industrially viable. Based on these, work is currently underway to particularly design more efficient white emitting hybrid materials by modification of the synthetic approach. The ability to use them as potential phosphors for SSL will be more specifically studied. White-emitting hybrid silica-based materials comprising lanthanide ions have been rarely reported to date.[49,55]

Acknowledgements

We wish to thank the China Scholarship Council (CSC) for a fellowship to XH (PhD grant), Dr Catherine Henry de Villeneuve for her assistance in recording IR spectra, Dr Thierry Gacoin for a facilitated access to the TGA analyzer, and the CNRS and the Ecole polytechnique for financial support, as well as the Labex CHARMMMAT.

Notes and references

[a] *Laboratoire de Chimie Moléculaire, UMR 9168 CNRS, Ecole polytechnique, Route de Saclay, 91128 Palaiseau Cedex, France.*
[b] *Laboratoire de Physique des Interfaces et des Couches Minces, UMR 7647 CNRS, Ecole polytechnique, Route de Saclay, 91128 Palaiseau Cedex, France.* [*] *Correspondence to: Gaël Zucchi, LPICM, UMR 7647 CNRS, Ecole polytechnique, Route de Saclay, 91128 Palaiseau Cedex, France. Email: gael.zucchi@polytechnique.edu.*
[c] *Institut d'Alembert, PPSM, CNRS UMR 8531, ENS Cachan, 61 Avenue du Président Wilson, 94235 Cachan, France.*
[d] *LICSEN, CEA Saclay IRAMIS/NIMBE, 91191 Gif Sur Yvette, France.*

1 A.-L. Pénard, T. Gacoin, J.-P. Boilot, *Acc. Chem. Res.* 2007, **40**, 895.
2 R. Pardo, M. Zayat, D. Levy, *Chem. Soc. Rev.* 2011, **40**, 672.
3 K. Matsukawa, *J. Photopolym. Sci. Technol.* 2005, **18**, 203.
4 G. Zucchi, V. Murugesan, D. Tondelier, D. Aldakov, T. Jeon, F. Yang, P. Thuéry, M. Ephritikhine, B. Geffroy, *Inorg. Chem.* 2011, **50**, 4851.
5 J. Kai, M. C. F. C. Felinto, L. A. O. Nunes, O. L. Malta, H. F. Brito, *J. Mater. Chem.* 2011, **21**, 3796.
6 H. F. Jiu, J. J. Ding, Y. Y. Sun, J. Bao, C. Gao, Q. J. Zhang, *J. Non-Cryst. Solids* 2006, **352**, 197.
7 J. Graffion, A. M. Cojocariu, X. Cattoen, R. A. S. Ferreira, V. R. Fernandes, P. S. Andre, L. D. Carlos, M. Wong Chi Man, J. R. Bartlett, *J. Mater. Chem.* 2012, **22**, 13279.
8 X. M. Guo, J. L. Canet, D. Boyer, P. Adumeau, R. Mahiou, *J. Sol-Gel Sci. Technol.* 2012, **64**, 404.
9 J. Graffion, X. Cattoën, M. Wong Chi Man, V. R. Fernandes, P. S. André, R. A. S. Ferreira, L. D. Carlos, *Chem. Mater.* 2011, **23**, 4773.

10 P. Lenaerts, A. Storms, J. Mullens, J. D'Haen, C. Görller-Walrand, K. Binnemans, K. Driesen, *Chem. Mater.* 2005, **17**, 5194.
11 L.D. Carlos, R. A. S. Ferreira, V. de. Z. Bermudez, B. Julian-Lopez, P. Escribano, *Chem. Soc. Rev.* 2011, **40**, 536.
12 S. Li, H. Song, W. Li, X. Ren, S. Lu, G. Pan, L. Fan, H. Yu, H. Zhang, R. Qin, Q. Lin, T. Wang, *J. Phys. Chem. B* 2006, **110**, 23164.
13 L. D. Carlos, R. A. S. Ferreira, V. de. Z. Bermudez, S. J. L. Ribeiro, *Adv. Mater.* 2009, **21**, 509.
14 L. Armelao, S. Quici, F. Barigelletti, G. Accorsi, G. Bottaro, M. Cavazzini, E. Tondello, *Coord. Chem. Rev.* 2010, **254**, 487.
15 Q. Xu, L. Li, B. Li, J. Yu, R. Xu, *Microp. Mesop. Mater.* 2000, **38**, 351.
16 Q. Xu, L. Li, X. Liu, R. Xu, *Chem. Mater.* 2002, **14**, 549.
17 L. Armelao, G. Bottaro, S. Quici, M. Cavazzini, C. Scalera, G. Accorsi, *Dalton Trans.* 2011, **40**, 11530.
18 J. Feng, H. Zhang, *Chem. Soc. Rev.* 2013, **42**, 387.
19 P. Escribano, B. Julian-Lopez, J. Planelles-Arago, E. Cordoncillo, B. Viana, C. Sanchez, *J. Mater. Chem.* 2008, **18**, 23.
20 X. Huang, Q. Wang, X. Yan, J. Xu, W. Liu, Q. Wang, Y. Tang, *J. Phys. Chem. C* 2011, **115**, 2332.
21 F. Artizu, F. Quochi, M. Saba, D. Loche, M. L. Mercuri, A. Serpe, A. Mura, G. Bongiovanni, P. Deplano, *Dalton Trans.* 2012, **41**, 13147.
22 B. Francis, D. B. Ambili Raj, M. L. P. Reddy, *Dalton Trans.* 2010, **39**, 8084.
23 Y. Li, B. Yan, H. Yang, *J. Phys. Chem. C* 2008, **112**, 3959.
24 J. Xu, L. Jia, Y. Ma, X. Liu, H. Tian, W. Liu, Y. Tang, *Mater. Chem. Phys.* 2012, **136**, 112.
25 H. Wang, Y. Ma, H. Tian, N. Tang, W. Liu, Y. Tang, *Dalton Trans.* 2010, **39**, 7485.
26 Q.-P. Li, B. Yan, *Dalton Trans.* 2012, **41**, 8567.
27 K. Binnemans, *Chem. Rev.* 2009, **109**, 4283.
28 G. M. Kloster, C.M. Taylor, S. P. Watton, *Inorg. Chem.* 1999, **38**, 3954.
29 A. Sergent, G. Zucchi, R. B. Pansu, M. Chaigneau, B. Geffroy, D. Tondelier, M. Ephritikhine, *J. Mater. Chem. C* 2013, **1**, 3207.
30 L. R. Melby, N. J. Rose, E. Abramson, J. C. Caris, *J. Am. Chem. Soc.* 1964, **86**, 5117.
31 J. C. de Mello, H. F. Wittmann, R. H. Friend, *Adv. Mater.* 1997, **9**, 230.
32 B. Samuneva, L. Kabaivanova, G. Chernev, P. Djambaski, E. Kashchieva, E. Emanuilova, I. M. M. Salvado, M. H. V. Fernandes, A. Wu, *J. Sol-Gel Sci. Technol.* 2008, **48**, 73.
33 J. L. Liu, B. Yan, *J. Phys. Chem. B* 2008, **112**, 10898.
34 G. Zucchi, O. Maury, P. Thuéry, M. Ephritikhine, *Inorg. Chem.* 2008, **47**, 10398.
35 Z. Chen, Y. Wu, F. Huang, D. Gu, F. Gan, *Spectrochim. Acta Part A: Mol. Biomol. Spec.* 2007, **66**, 1024.
36 R. C. Evans, P. C. Marr, *Chem. Commun.* 2012, **48**, 3742.
37 J.-C. G. Bünzli, *Lanthanides Probes in Life, Chemical and Earth Sciences : Theory and Pratice*, Elsevier, Amsterdam 1989.
38 P. A. Tanner, *Chem. Soc. Rev.* 2013, **42**, 5090.
39 S. V. Eliseeva, D. N. Pleshkov, K. A. Lyssenko, L. S. Lepnev, J.-C. G. Bünzli, N. P. Kuzmina, *Inorg. Chem.* 2011, **50**, 5137.
40 S. Mohapatra, C. Adhikari, H. Riju, T. K. Maji, *Inorg. Chem.* 2012, **51**, 4891.
41 S, Biju, Y. K. Eom, J.-C.G. Bünzli, H.K. Kim, *J. Mater. Chem. C* 2013, **1**, 3454
42 A. Voloshin, N. Shavaleev, V. Kazakov, *J. Lumin.* 2000, **91**, 49.
43 G. Zucchi, A.-C. Ferrand, R. Scopelliti, J.-C. G. Bünzli, *Inorg. Chem.* 2002, **41**, 2459.
44 T. Ogi, Y. Kaihatsu, F. Iskandar, W.-N. Wang, K. Okuyama, *Adv. Mater.* 2008, **20**, 3235.
45 K. M. Lee, K. W. Cheah, B. L. An, M. L. Gong, Y. L. Liu, *Appl. Phys. A* 2005, **80**, 337.
46 P. He, H. H. Wang, H. G. Yan, W. Hu, J. X. Shi, M. L. Gong, *Dalton Trans.* 2010, **39**, 8919.
47 G. Shao, H. Yu, N. Zhang, Y. He, K. Feng, X. Yang, R. Cao, M. Gong, *Phys. Chem. Chem. Phys.* **2014**, *16*, 695
48 H. Yan, H. Wang, P. He, J. Shi, M. Gong, *Synth. Met.* 2011, **161**, 748.
49 T. Wang, P. Li, H. Li, *ACS Appl. Mater. Interfaces* 2014, **6**, 12915.
50 J. Xu, Y. Ma, L. Jia, X. Huang, Z. Deng, H. Wang, W. Liu, Y. Tang, *Mater. Chem. Phys.* 2012, **133**, 78.
51 M. Fernandes, V. de Zea Bermudes, R.A. Sa Ferreira, L.D. Carlos, A. Charas, J. Morgado, M. M. Silva, M. J. Smith, *Chem. Mater.* 2007, **19**, 3892.
52 T. Fukuda, S. Kato, S. Akiyama, Z. Honda, N. Kamata, *Opt. Mater.* 2012, **35**, 5.
53 L. Armarelo, G. Bottaro, S. Quici, M. Cavazzini, M. C. Raffo, F. Barigelletti, G. Accorsi, *Chem. Commun.* 2007, 2911.
54 D. Zhao, S.-J. Seo, B.-S. Bae, *Adv. Mater.* 2007, **19**, 3473.
55 L. Armarelo, G. Bottaro, S. Quici, C. Scalera, M. Cavazzini, G. Accorsi, M. Bolognesi, *ChemPhysChem* 2010, **11**, 2499.